

A molecular basis for polymer flammability

Richard E. Lyon^{a,*}, Michael T. Takemori^b, Natallia Safronava^c, Stanislav I. Stoliarov^c, Richard N. Walters^a

^a Federal Aviation Administration, Airport and Aircraft Safety R&D Division, William J. Hughes Technical Center, Atlantic City International Airport, NJ 08405, USA

^b GE Global Research, Niskayuna, NY, USA

^c SRA International, Linwood, NJ, USA

ARTICLE INFO

Article history:

Received 5 February 2009

Received in revised form

16 March 2009

Accepted 18 March 2009

Available online 7 April 2009

Keywords:

Polymer

Combustion

Flammability

ABSTRACT

Empirical molar group contributions to the thermal combustion properties measured by microscale combustion calorimetry were determined by multiple linear regression of data for engineering polymers of known chemical composition. Char yield, heat of combustion and heat release capacity of polymers calculated from their chemical structure using optimized additive molar group contributions were in reasonable agreement with measured values for these properties. The relationship between the thermal combustion properties and the results of standardized flame and fire tests (i.e., flammability) was examined statistically for an expanded data set.

Published by Elsevier Ltd.

1. Introduction

A molecular basis for polymer flammability exists if there are *material properties* that govern flammability and are rooted in the chemical structure of the polymer and are amenable to exact measurement [1]. Material properties are distinct from *product properties* measured in flame and fire tests [2]. Product properties depend on extrinsic factors such as the size of the sample, its method of fabrication, the sample processing history, physical processes induced by burning such as swelling or dripping, chemical processes in the flame, and the characteristics of the test method [3–7]. Consequently, standardized tests are needed to compare product fire properties. Bench-scale fire calorimeters are standardized tests that measure the fire response of a product such as its heat release rate, smoke production, and ignition delay. Flame resistance, which is the tendency of a thin strip of material to resist burning after brief ignition by a small flame, is another product property that is sensitive to extrinsic factors [8]. In this paper, a molecular basis for polymer flammability is established by demonstrating that there are material properties rooted in the polymer chemical structure that correlate fire and flame test results.

2. Approach

The largest unique chemical descriptors of polymers are their repeat units that are comprised of chemical groups/moieties such

as methyl, phenyl, carbonyl, ether, amide, and ester. These chemical groups represent a relatively tractable set for purposes of computing polymer properties [1,9–11]. A higher level of detail considers atomistic contributions to polymer properties either empirically [12] or fundamentally [13], but these require a significant computational effort to account for atomic interactions.

A relatively simple approach to calculate an intrinsic property of a polymer from its chemical groups is to assume that groups *i* and *j* contribute an amount P_{ij} to a property *P* according to a weighted sum over all of the pair-wise interactions between *n* groups [1]. If ϕ_{ij} is a dimensionless weighting factor for the interaction between groups *i* and *j*:

$$P = \sum_{i=1}^n \sum_{j=1}^n \phi_{ij} P_{ij} = \sum_{i=j} \phi_{ij} P_{ij} + \sum_{i \neq j} \phi_{ij} P_{ij}$$

$$= (\phi_{11} P_{11} + \phi_{22} P_{22} + \phi_{33} P_{33} + \dots) + (\phi_{12} P_{12} + \phi_{21} P_{21} + \phi_{13} P_{13} + \phi_{31} P_{31} + \phi_{23} P_{23} + \phi_{32} P_{32} + \dots) \quad (1)$$

The order of the subscripts *i* and *j* is interchangeable and using contracted notation, $\phi_{ii} = \phi_i$ and $P_{ii} = P_i$

$$P = \sum \phi_i P_i + 2 \sum_{i=1} \sum_{j=i+1} \phi_{ij} P_{ij}$$

$$= (\phi_1 P_1 + \phi_2 P_2 + \phi_3 P_3 + \dots) + (2\phi_{12} P_{12} + 2\phi_{13} P_{13} + 2\phi_{23} P_{23} + \dots) \quad (2)$$

If the weighting factors are defined to be the geometric mean of the mole, mass or volume fractions of the components x_i multiplied

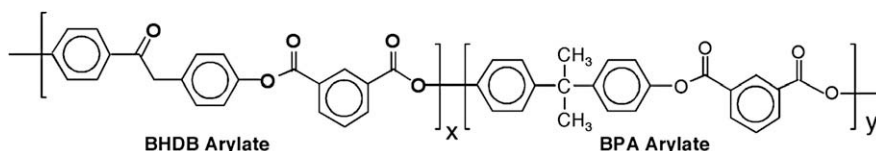
* Corresponding author.

E-mail address: richard.e.lyon@faa.gov (R.E. Lyon).

by an interaction parameter λ_{ij} that describes the strength of the pair-wise interaction between groups i and j , then $\phi_{ij} = \lambda_{ij}(x_i x_j)^{1/2}$. Furthermore, if P_{ij} is the arithmetic mean of the properties, $P_{ij} = (P_i + P_j)/2$, and $\lambda_{ii} \equiv 1$

$$P = \sum x_i P_i + \sum_{i=1} \sum_{j=i+1} \lambda_{ij} x_i x_j P_{ij}$$

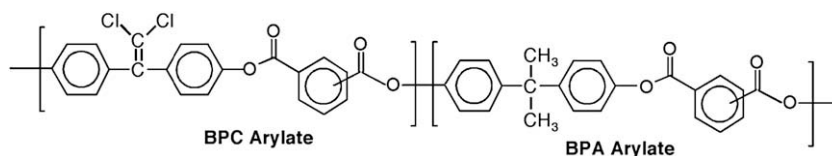
$$= x_1 P_1 + x_2 P_2 + x_3 P_3 + \dots + \lambda_{12} (x_1 x_2)^{1/2} (P_1 + P_2) + \lambda_{13} (x_1 x_3)^{1/2} (P_1 + P_3) + \lambda_{23} (x_2 x_3)^{1/2} (P_2 + P_3) + \dots \quad (3)$$



The pair-wise interaction terms λ_{ij} in Equation (3) can produce positive or negative deviations from additivity. For a simple two-component mixture or compound, $n = 2$, and Equation (3) becomes

$$P = x_1 P_1 + x_2 P_2 + \lambda_{12} (x_1 x_2)^{1/2} (P_1 + P_2) \quad (4)$$

Equation (4) is plotted in Fig. 1 to show the effect of the sign and magnitude of an interaction term having values $\lambda_{ij} = -1/2, 0$, and $1/2$



on P for a two-component mixture where $x_1 + x_2 = 1$, and for which $P_1 = 2P_2$. Positive deviation from additivity (synergism) is observed for $\lambda_{12} = \lambda > 0$ and negative deviation (antagonism) for $\lambda < 0$.

When all of the interaction parameters in Equation (3) equal zero (i.e., $\lambda_{ij} = 0$), the simple rule of mixtures (additivity) is obtained and this is plotted as the straight line in Fig. 1,

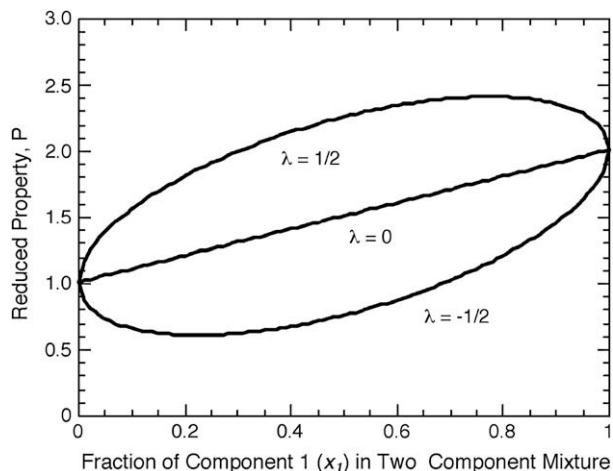


Fig. 1. Reduced property P of binary mixture versus fraction of component 1 for $P_1 = 2P_2$.

$$P = x_1 P_1 + x_2 P_2 + x_3 P_3 + \dots x_n P_n \quad (5)$$

Examples from the literature show that Equation (4) provides a reasonable description of the properties of binary mixtures using λ as the sole adjustable parameter. Fig. 2 is a plot of the mass fraction of char (char yield) remaining after pyrolysis at 850 °C versus the mass fraction of the bishydroxydeoxybenzoin (BHDB)-based polyarylate (arylate) repeat unit in a copolyarylate with bisphenol-A [14]. The solid line is the best fit of Equation (4) to the data with $\lambda = 0$ in Equation (4) for the copolymer (i.e., Equation (5)).

It is clear that the char yields of the BHDB and BPA arylate moieties are additive, and that Equation (5) describes the data for this copolymer reasonably well with correlation coefficient $R = 0.96$.

If BHDB is replaced with 1,1-dichloro-2,2-bis(4-hydroxyphenyl)ethylene/bisphenol-C/BPC in polyarylate copolymers and blends [15],

Fig. 3 is a plot of char yield versus mass fraction of BPC arylate in BPC–BPA copolyarylates and blends of BPC polyarylate with BPA polyarylate. Synergism between BPC and BPA with respect to char yield is observed when BPC is incorporated into the mixture as either a co-monomer or blended polymer as evidenced by the positive deviation from additivity with $\lambda = 0.24$ obtained by

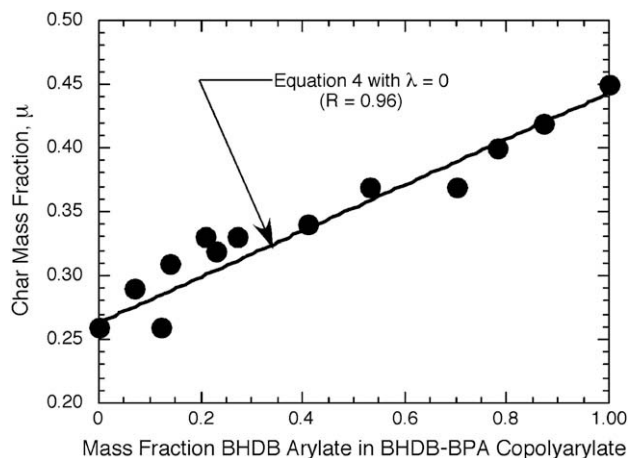


Fig. 2. Mass fraction of char in BHDB–BPA copolyarylate versus mole fraction of BHDB arylate. Solid line is best fit of Equation (4) ($\lambda = 0$).

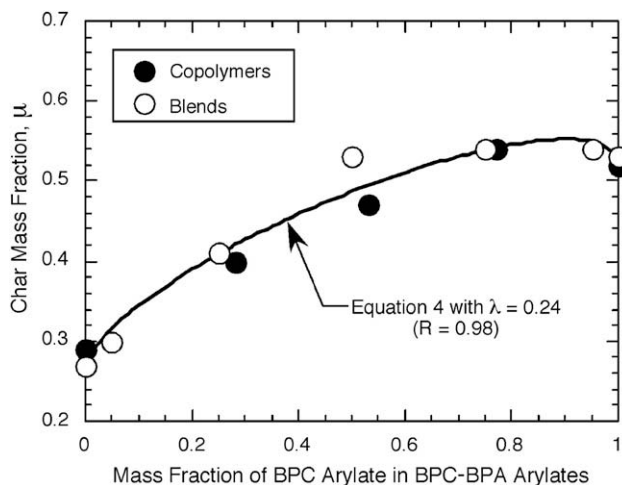


Fig. 3. Mass fraction of char in BPC-BPA arylate copolymers and blends versus mass fraction of BPC arylate. Solid line is best fit of Equation (4) ($\lambda = 0.24$).

a non-linear least squares regression of Equation (4) on the experimental data with $R = 0.98$.

Copolyarylates based on BHDB have been synthesized and characterized in which a phosphonate moiety replaces the terephthalate moiety in the polymer backbone [16,17].

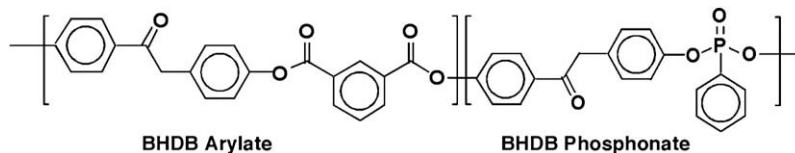


Fig. 4 shows the results for char yield versus composition for the BHDB arylate-co-phosphonate. Synergy is observed with $\lambda = 0.13$, obtained from a non-linear least squares regression of Equation (4) on the experimental data with $R = 0.95$.

Despite the ability of the generalized chemical interaction model (i.e., Equation (3)) to describe properties of two-component systems with a single adjustable parameter λ (Figs. 2–4), the number of undetermined coefficients rapidly

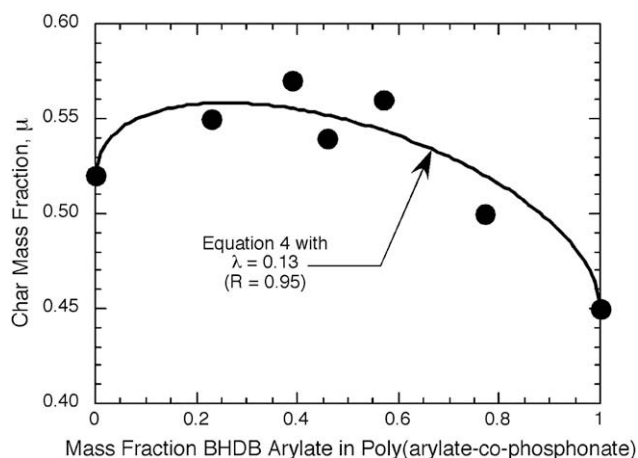


Fig. 4. Mass fraction of char in BHDB polyarylate-co-phosphonate versus mass fraction of BHDB arylate. Solid line is best fit of Equation (4) ($\lambda = 0.13$).

becomes intractable when polymer repeat units are subdivided into their constituent chemical groups and λ_{ij} must be computed along with P_i for $n > 2$ components. For this reason, and at the expense of generality, the interaction terms in Equation (3) are usually neglected and additivity (Equation (5)) is assumed for chemical groups on a molar basis, i.e., molar additivity [1]. Thus, if $x_i = n_i$ is the mole fraction of component i having molar group contribution P_i , then the molar quantity \mathbf{P} is obtained by additivity

$$\mathbf{P} = \sum n_i P_i \quad (6)$$

The specific (mass based) property \mathbf{p} is obtained from \mathbf{P} by dividing by the molar mass of the polymer repeat unit \mathbf{M} . Thus, if N_i and M_i are the number of moles and the molar mass of component i , respectively,

$$\mathbf{p} = \frac{\mathbf{P}}{\mathbf{M}} = \frac{\sum n_i P_i}{\sum n_i M_i} = \frac{\sum N_i P_i}{\sum N_i M_i} \quad (7)$$

Equation (7) has been used to calculate dozens of polymer properties [1], including several that are related to their flammability [1,10,11], from additive molar contributions of the chemical groups comprising the polymer repeat unit. Additive flammability properties that are related to the chemical structure include the heat of complete combustion of the fuel gases H_c [11,18] as well as solid properties such as heat capacity, thermal conductivity, density,

thermal decomposition (ignition) temperature T_p , activation energy for pyrolysis E_a [1], char yield μ [1,11], and the tendency to form soot in a diffusion flame [19].

It follows that if a property is a combination of intrinsic properties it should be calculable from the same (or similar) chemical groups as the component properties. The capacity of a solid to release combustion energy in a single-step thermal decomposition process during a linear temperature program at constant heating rate is a unique combination of thermal combustion properties called the heat release capacity, η_c having units of J/g K [20–22]

$$\eta_c = \frac{H_c(1 - \mu)}{eRT_p^2/E_a} = \frac{h_c}{\Delta T_p} \quad (8)$$

In Equation (8), $(1 - \mu)$ is the volatile fuel fraction, $h_c = H_c(1 - \mu)$ is the heat of complete combustion of the pyrolysis gases per unit initial mass of solid, $\Delta T_p = eRT_p^2/E_a$ is the pyrolysis temperature interval, and e and R are the natural number and gas constant, respectively. Since each of the thermal combustion properties on the right hand sides of Equation (8) is calculable from additive molar group contributions, the heat release capacity itself should be calculable from additive molar quantities [10,11]. Thus, if Ψ is the molar heat release capacity and ψ_i are the molar contributions of components i .

$$\Psi = \sum n_i \psi_i \quad (9)$$

The mass-based heat release capacity η_c in Joules per gram of sample per degree of temperature rise (J/g K) is

$$\eta_c = \frac{\sum N_i \Psi_i}{\sum N_i M_i} \quad (10)$$

The heat of combustion of the sample gases, h_c (J/g-sample) is likewise obtained from molar group contributions Ω_i

$$h_c = \frac{\sum N_i \Omega_i}{\sum N_i M_i} \quad (11)$$

The mass fraction of char μ (g-char/g-sample) is also obtained from its molar group contributions X_i ,

$$\mu = \frac{\sum N_i X_i}{\sum N_i M_i} \quad (12)$$

It is well known that the flammability of polymers is related to their thermal and combustion properties and that these thermal combustion properties are amenable to calculation by additive molar group contributions [1,9–11]. In the present study we recalculate additive molar group contributions to η_c for the chemical groups specific to engineering plastics, add values for h_c and μ , and compare the predictions to experimental values. Reasonable agreement between measured thermal combustion properties and those calculated using the additive model (i.e., neglecting chemical group interactions) is observed, reinforcing the concept that these thermal combustion properties are material properties. Finally, we examine the effect of these thermal combustion properties on polymer flammability as measured in standard tests using a probabilistic, rather than deterministic, analysis of an expanded data set.

3. Experimental

3.1. Materials

Polymers that were tested to determine molar group contributions include 73 research polymers synthesized at laboratory scale and 11 commercial thermoplastic polymers obtained in sheet form from plastics suppliers without additives. The 11 commercial thermoplastics were included in the flame and fire test population for which thermal combustion properties were also measured. The sample population for flame, fire and thermal combustion property (flammability) tests includes 69 thermosetting and thermoplastic hydrocarbon polymers and polymer blends, 26 halogenated polymers or polymers containing halogenated flame retardants, 30 polymers containing non-halogen (typically phosphorus) flame retardants, and 35 polymer composites reinforced with particulate mineral fillers, glass fibers, carbon fibers or nanometer-sized clay obtained from commercial sources and research laboratories over a period of several years [23–28]. Thus, hydrocarbon polymers account for 43% of the flammability sample population, halogen-containing polymers account for 16%, non-halogen flame retardant plastics 19% and composites 22%. Methane, oxygen, and nitrogen gases used for calibration and testing were dry, ultra high purity (>99.5%) grades obtained from Matheson Gas Products.

3.2. Methods

3.2.1. Microscale combustion calorimetry

Thermal combustion properties were measured using microscale combustion calorimetry (MCC) according to a standard method [29]. In the MCC test a 3–5 mg specimen is heated at

a constant rate $\beta = 1$ K/s from ambient temperature to 850 °C in nitrogen flowing at 80 cm³/min. The pyrolysis gases are purged from the sample chamber by the nitrogen, mixed with excess oxygen, and completely combusted at 900 °C for 10 s. The specific heat release rate during the test $Q(t)$ in units of Watts per gram of sample is calculated from the flow rate of the gas stream and the oxygen consumed by combustion of the pyrolysis gases. The sample is weighed before and after the test to determine the initial and residual mass. Four thermal combustion properties are deduced from the specific heat release rate history during the typical 15 min test: the total heat released by combustion of fuel gases per unit mass of sample h_c (kJ/g), the temperature T_p (K) at the maximum specific heat release rate of the sample, the heat release capacity of the sample η_c (J/g K), and the pyrolysis residue φ (g/g-sample) which includes the weight of the polymer char μ and any inert material remaining after the test at 850 °C.

Samples containing components that thermally decompose at distinctly different temperatures can exhibit specific heat release rate histories with multiple peaks. The components that give rise to multiple peaks may be chemical moieties present in the original polymer, volatile additives, or chemical intermediates generated during the decomposition process. In these cases, the thermal combustion properties of the sample are weighted averages of the component values. If w_i , h_i and Q_i^{\max} are the mass fraction, combustion heat, and maximum specific heat release rate of component i , respectively, in an n -component mixture or compound, the specific combustion heat of the compound is given by the energy balance:

$$h_c = w_1 h_1 + w_2 h_2 + \dots + w_n h_n = \sum_{i=1}^n w_i h_i \quad (13)$$

The pyrolysis temperature interval of the compound ΔT_p is computed from the pyrolysis temperature intervals of the components ΔT_i using a lower bound rule of mixtures with $\phi_i = w_i h_i / h_c$ a weighting factor and $\sum \phi_i = 1$ by Equation (13),

$$\frac{1}{\Delta T_p} = \sum_{i=1}^n \frac{\phi_i}{\Delta T_i} = \sum_{i=1}^n w_i \frac{h_i / h_c}{\Delta T_i} = \frac{1}{h_c} \sum_{i=1}^n w_i \frac{h_i}{\Delta T_i} \quad (14)$$

Equations (8) and (14) give the heat release capacity of a compound containing n -components in terms of the maximum specific heat release rates of the components normalized for sample mass and heating rate, $q_i^{\max} = w_i Q_i^{\max} / \beta = w_i \eta_i$.

$$\eta_c = \frac{h_c}{\Delta T_p} = \sum_{i=1}^n w_i \frac{h_i}{\Delta T_i} = \sum_{i=1}^n w_i \eta_i \sum_{i=1}^n q_i^{\max} \quad (15)$$

In practice, η_c is determined by summing the minimum number of Gaussian, Lorentzian, asymmetric Gaussian or Lorentzian, or asymmetric Gaussian–Lorentzian hybrid peaks needed to fit the specific heat release rate history measured in the MCC with an accuracy of at least 90%. Fig. 5 shows $q(T)$ versus temperature for a blend of 75 weight percent polycarbonate (PC) and 25 weight percent acrylonitrile–butadiene–styrene terpolymer (ABS). The solid lines are the asymmetric Gaussian–Lorentzian peak fits of the ABS and PC components assuming $n=2$ for the blend, which reproduce the MCC data with sufficient accuracy. From the individual peak fits, $q_{\text{ABS}}^{\max} = 170$ J/g K and $q_{\text{PC}}^{\max} = 370$ J/g K, so the heat release capacity of the PC/ABS blend is $\eta_c = q_{\text{ABS}}^{\max} + q_{\text{PC}}^{\max} = 540$ J/g K. Fitting an additional peak to the small shoulder at 490 °C does not change η_c significantly because the ABS and PC peaks' heights are correspondingly reduced to conserve the total heat of combustion h_c as per Equation (13). The heat release capacities of the pure PC

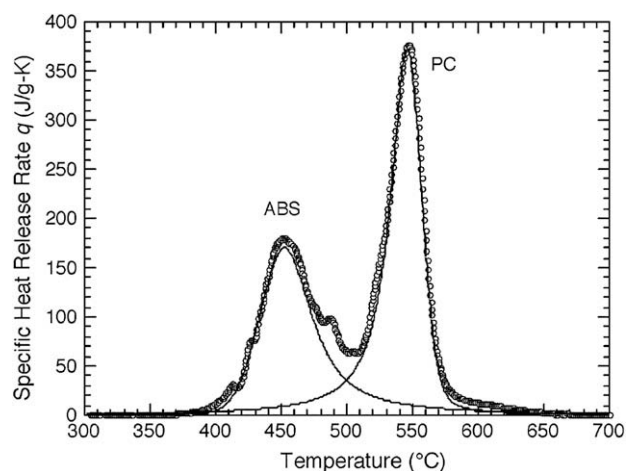


Fig. 5. MCC data for 75/25 (w/w) PC/ABS blend. Circles are experimental data. Solid lines are asymmetric Gaussian-Lorentzian fits of the ABS and PC peaks.

and ABS can be calculated from the specific heat release rates of these 2 components in the blend and their nominal mass fractions:

$$\begin{aligned}\eta_{\text{ABS}} &= q_{\text{ABS}}^{\text{max}}/w_{\text{ABS}} \\ &= (170 \text{ J/g-blend/K})/(0.25 \text{ g-ABS/g-blend}) \\ &= 680 \text{ J/g-ABS/K}\end{aligned}$$

$$\begin{aligned}\eta_{\text{PC}} &= q_{\text{PC}}^{\text{max}}/w_{\text{PC}} = (370 \text{ J/g-blend/K})/(0.75 \text{ g-PC/g-blend}) \\ &= 493 \text{ J/g-PC/K}\end{aligned}$$

These values compare reasonably well to the measured values for the pure components, $\eta_{\text{ABS}} = 690 \pm 20 \text{ J/g K}$ and $\eta_{\text{PC}} = 511 \pm 33 \text{ J/g K}$.

The heat of combustion and heat release capacity of polymers containing inert filler or noncombustible fiber are reduced in proportion to the combustible mass of the sample. For example, the heat release capacity of polyhexamethylenedipamide (PA66) containing 33 weight percent glass fiber reinforcement can be calculated from the mass fractions and heat release capacities of the pure components. The heat release capacity of PA66 is $\eta_{\text{PA66}} = 615 \pm 15 \text{ J/g K}$ [23] while the heat release capacity of the noncombustible fiberglass is $\eta_{\text{glass}} = 0 \text{ J/g K}$, so the heat release capacity of the glass fiber reinforced polyamide plastic (GFRP) should be

$$\begin{aligned}\eta_{\text{GFRP}} &= (w_{\text{glass}})(\eta_{\text{glass}}) + (w_{\text{PA66}})(\eta_{\text{PA66}}) \\ &= (0.33)(0) + (0.67)(615 \text{ J/g K}) = 412 \pm 15 \text{ J/g K}.\end{aligned}$$

This value is within the experimental error of the measured value for the compound, $\eta_{\text{GFRP}} = 390 \pm 14 \text{ J/g K}$.

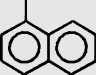
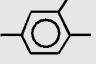
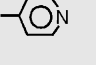
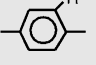
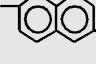
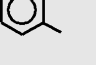
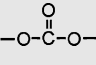
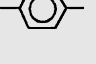


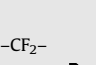
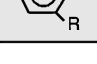
Table 1
Classification criteria for the Underwriters Laboratory Vertical Test for Flammability of Plastics (UL 94V) [30,31].

Criterion	UL 94 classification		
	V-0	V-1	V-2
Flaming combustion time after test flame removed (s)	≤10	≤30	≤30
Total flaming time for 5 specimens (s)	≤50	≤250	≤250
Flaming/glowing combustion up to the clamp?	No	No	No
Flaming drops ignite cotton 300 mm below test specimen?	No	No	Yes
Glowing persists for more than 30 s after test flame?	No	≤60	≤60

3.2.2. Vertical flame testing

The propensity for vertical burning under ambient conditions was measured on 3 mm × 13 mm × 125 mm plastic samples according to a standard method [30,31]. The procedure consists of subjecting a set of 5 preconditioned specimens to a standard Bunsen burner test flame for two, successive, 10-s flame

Table 2a
Molar group contribution values.

Chemical group ^a	Type ^b	Molar group contributions			$\Psi_i/M_i \text{ J/g K}$
		$\Omega_i \text{ MJ/mol}$	$X_i \text{ g/mol}$	$\Psi_i \text{ kJ/mol K}$	
-C(CH ₃) ₂ -	B	2.63	0	85.5	2036
-CH ₃	S	0.50	0	18.5	1233
-CH ₂ -	B	0.51	0	14.4	1029
	S	4.84	0	108.6	855
-O-	B	0.12	0	11.1	694
	B	2.19	21	43.2	576
	S	2.16	0	39.6	508
-CH-	S	0.67	0	5.7	438
-NH-	B	0.72	0	6.1	407
	S, B	1.69	21	24.7	329
	B	2.38	54	39.6	314
	B	-0.69	76	23.0	303
-OH	S	-0.12	0	4.8	282
-S-	B	0.78	9	7.9	247
	B	0.22	-1	13.6	227
-CH ₂ O-	B	0.42	0	5.8	193
	B	1.08	35	13.1	172
	B	1.08	35	13.1	172
	S	1.49	37	12.5	162
	B	0.24	0	3.1	70
-CF ₂ -	B	0.15	2	2.5	50
	S, B	1.20	48	0.4	5

applications. The duration of flaming (after-flame time) is recorded after the first flame application and the after-flame and afterglow times are recorded following the second flame application for each specimen. Information is also recorded on whether or not flaming drops of molten plastic fall from the specimen and whether or not these drops ignite a cotton indicator. The total flame time is recorded for each 5-specimen set. A qualitative classification of the flame resistance of the material is made according to the criteria given in Table 1.

Table 2b
Additional molar group contribution values.

Chemical group ^a	Type ^b	Molar group contributions			Ψ_i/M_i J/g K
		Δ_i MJ/mol	X_i g/mol	Ψ_i kJ/mol K	
	B	0.79	87	-1.0	-9
	B	0.19	128	-3.3	-21
-CF ₃	S	-0.96	40	-4.0	-58
-NH ₂	S	-0.04	1	-1.4	-88
	S, B	0.13	0	-1.7	-121
	B	-0.04	100	-18.6	-128
	B	0.25	129	-27.7	-129
	S	0.27	96	-17.3	-165
	B	0.31	-1	-10.9	-170
	S	-0.07	3	-13.5	-307
-Cl	S	-0.47	11	-11.8	-333
	S	-1.26	79	-33.3	-351
	S	1.00	-2	-5.3	-442
	B	-0.19	7	-12.6	-450
-C≡N	S	-1.85	26	-36.6	-1408
	B	-0.81	28	-98.5	-3518

^a R = Organic substituent.

^b B = Backbone group, S = Side or pendant group.

3.2.3. Fire testing

Fire testing was performed on 10 cm × 10 cm square samples ranging in thickness from 1.6 to 6 mm according to a standard method [32] using an edge frame holder and an irradiance of 50 kW/m² (Cone Calorimeter, Fire Testing Technology).

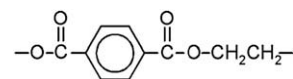
4. Results and discussion

4.1. Molar group contributions

Empirical molar group contributions to the thermal combustion properties were determined by multiple linear regression of the thermal combustion properties: η_c , h_c , and μ measured by MCC against 38 backbone and side-group component chemical groups using a commercial spreadsheet program [11]. Earlier efforts had established the efficacy of molar group contributions to η_c for a wide range of thermosetting and thermoplastic polymers [10]. In the present study, the molar group contributions were re-optimized to better fit the focal subclass of engineering plastics comprised mostly of polycarbonates and some polyester carbonates, and extended to include h_c and μ data. Data from over a hundred different formulations tested by MCC were used in the linear regression to provide the optimized set of molar group contributions in Tables 2a and 2b. The molar group contributions to the heat release capacity Ψ_i were normalized by the molar mass of the chemical group and these specific values, listed in the last column of Table 2, were used to sort all of the group contributions to η_c . Scanning down the columns in Table 2 shows that chemical groups in engineering thermoplastics add to η_c in the approximate order: aliphatic > aromatic > heterocycles > heteroatoms as the contributions to the heat of combustion (Δ_i) and the char yield (X_i) change in opposite directions with this ordering in accordance with Equation (8).

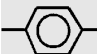
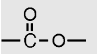
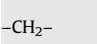
Negative values of the molar group contributions in Table 2 are a consequence of neglecting the interaction parameters of Equation (3) in the additive model of Equation (5). Large negative contributions to the heat release capacity by imidazole, oxazole and imide heterocycles and heteroatom groups in Table 2b reflect strong synergistic interactions between these and other groups in polymers that are not captured by simple additivity. For example, Fig. 3 demonstrates a strong positive (synergistic) interaction between BPC and BPA polyarylates with respect to char forming tendency that is attributable to the 1,1-dichloro-2,2-bis(ethylene) group (>C=C(Cl)₂) [33] and is expressed as negative contributions to the heat of combustion Δ and heat release capacity Ψ in the additive model (Table 2).

The thermal combustion properties of a polymer of known chemical structure can be calculated by summing the additive molar group contributions in Table 2 according to Equations (10)–(12). By way of example, the chemical structure of the repeat unit of polyethyleneterephthalate (PET) is,



The following data for the chemical groups comprising the PET repeat unit, their molar masses M_i and the corresponding molar group contributions are obtained from Table 2.

The thermal combustion properties are then computed from Equations (10)–(12) and compared to measured values [11,23,24] given in parentheses for this example.

Group	N_i	Molar quantity (P_i)			Ψ (kJ/mol K)
		M_i (g/mol)	Ω (MJ/mol)	X (g/mol)	
	1	76	1.08	35	13.1
	2	44	0.24	0	3.1
	2	14	0.51	0	14.4
$\sum N_i P_i$		192 g	2.58 MJ	35 g	48.1 kJ/K

$$h_c = \frac{\sum N_i \Omega_i}{\sum N_i M_i} = \frac{2.58 \text{ MJ}}{192 \text{ g}}$$

$$= 13.4 \text{ kJ/g (Measured values } \approx 16 \text{ kJ/g)}$$

$$\mu = \frac{\sum N_i X_i}{\sum N_i M_i} = \frac{35 \text{ g}}{192 \text{ g}} = 0.18 \text{ (Measured values } \approx 0.13)$$

$$\eta_c = \frac{\sum N_i \Psi_i}{\sum N_i M_i} = \frac{48.1 \text{ kJ/K}}{192 \text{ g}}$$

$$= 251 \frac{\text{J}}{\text{g K}} \text{ (Measured values } \approx 350 \text{ J/g K)}$$

Figs. 6 through 8 show the results for the thermal combustion properties modeled as additive molar functions versus measured values for the 73 experimental polymers and 11 commercial polymers using the 38 individual chemical groups.

Fig. 6 shows the modeled versus experimental char yield μ in the MCC and the least squares regression line calculated from the data and forced through the origin having slope 0.929 with $R = 0.95$. The experimental data are reasonably well approximated by additive molar contributions to charring (Tables 2a and 2b).

Fig. 7 shows the results of the additive model calculations of h_c versus the measured values for the 84 test polymers. The least squares regression line forced through the origin has slope 0.859 with $R = 0.88$.

The molar group contributions to η_c were refined from the previous set [10] and recalculated for the 84 experimental and commercial polymers in an attempt to obtain better predictive capability for the subset of engineering thermoplastics. The results of the additive model calculations for η_c are shown in

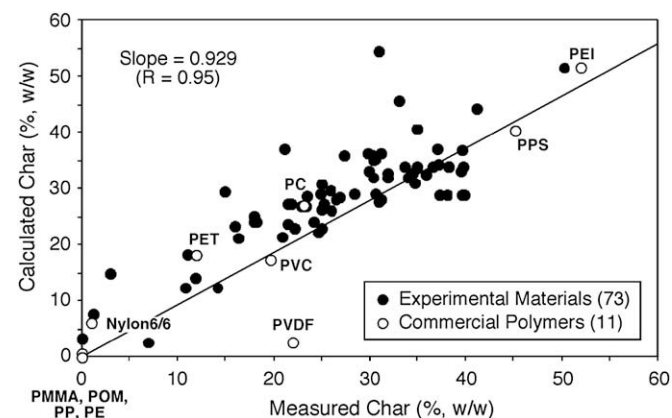


Fig. 6. Char yield μ calculated from the additive model versus measured μ for 84 polymers.

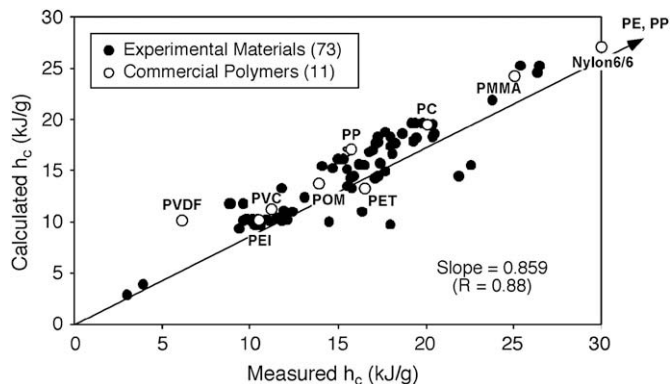


Fig. 7. Specific heat of combustion h_c calculated by the additive model versus measured h_c for 84 polymers.

Fig. 8 versus the measured values from MCC. The least squares regression line forced through the origin has slope 0.98 with $R = 0.88$.

4.2. Flammability and thermal combustion properties

The uncertainty in the results of standardized flame and fire tests due to systematic and random measurement errors, sample variations, and test procedures [3–8] precludes a deterministic analysis of the relationship between these product properties and polymer thermal combustion properties over a wide range of composition and fire behavior [22,25–27]. Moreover, macroscopic physical and chemical processes such as dripping, distortion, swelling, accumulation of char at the burning surface, intumescence and inhibition of flame chemistry that affect the results of flame and fire tests are not accounted for by the thermal combustion properties [22]. Further obscuring a molecular basis for flammability is the fact that imperfections in polymer chain architecture, impurities, additives, modifiers and flame retardants that change the thermal decomposition chemistry of polymers will change the thermal combustion properties in a way that is not presently calculable from the additive molar group contributions derived for pure polymers in Table 2. Consequently, and in view of the above limitations, an attempt was made to use a statistical rather than deterministic analysis to correlate the thermal combustion properties of materials with the results of flame and fire tests.

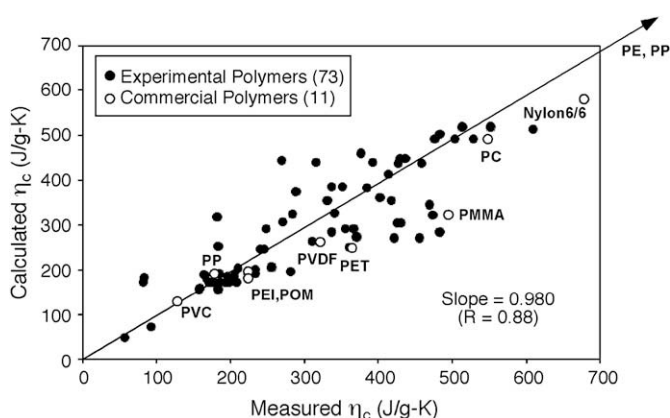


Fig. 8. Heat release capacity η_c calculated from additive molar group contribution model versus η_c measured in MCC for 84 polymers.

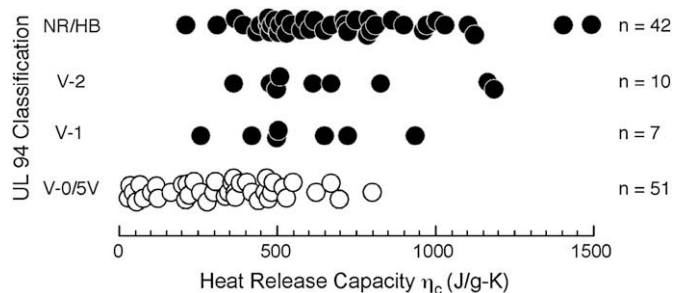


Fig. 9. UL 94 classification versus η_c for 110 polymers, plastics and composites. Solid circles are burn results. Open circles are no-burn results.

4.2.1. Flame test results

Qualitative vertical flame test results were converted to binary (burn/no-burn) results by assigning a burn rating to V-1, V-2, No Rating/NR and HB results and a no-burn rating to V-0 results. Fig. 9 shows UL 94 classification data for 110 samples versus the measured heat release capacity of the sample η_c . Open circles indicate a V-0 (no-burn) result while solid circles indicate a V-1, V-2, NR or HB (burn) result. The data in Fig. 9 were sorted by η_c and the fraction of burn results (probability of burning p_B) was computed for successive 10-sample bins along with the average η_c for the bin. The results of this sorting and binning procedure for the data in Fig. 9 are plotted in Fig. 10.

The probability of burning p_B versus the other thermal combustion properties measured in the MCC test were computed by the same sorting and binning procedure that was used for η_c , and the results are shown in Figs. 11–13. Fig. 11 shows the probability of burning versus the heat of combustion h_c for 110 polymers, plastics and composites using a 10-sample bin. The correlation between p_B and h_c is approximately the same as it is with η_c .

The probability of burning p_B , the pyrolysis residue φ (which includes both char, inorganic filler and fibrous reinforcement for plastics) and the temperature at peak pyrolysis rate T_p were computed for 77 of the 110 plastics for which these data were available. The results of these calculations for p_B and the average values of φ and T_p using a 7-sample bin are plotted in Figs. 12 and 13.

The data in Figs. 10–13 show that the trend of p_B with η_c and h_c is more nearly monotonic and better correlated than the trend with φ and T_p for the qualitative flame test results of UL 94V. Similar

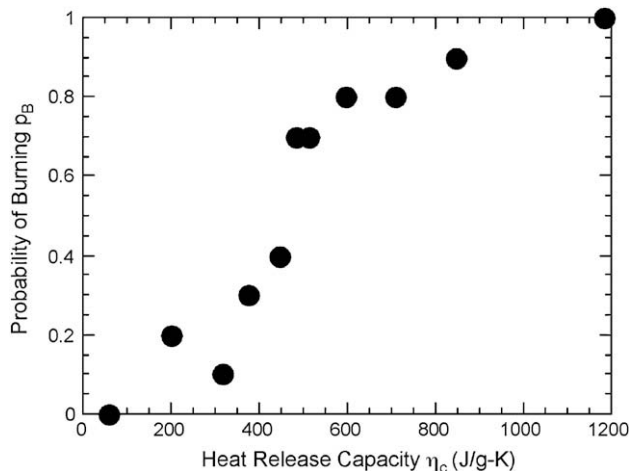


Fig. 10. The probability of burning (p_B) in the UL 94V test versus the heat release capacity (η_c) of 110 polymers, plastics and composites.

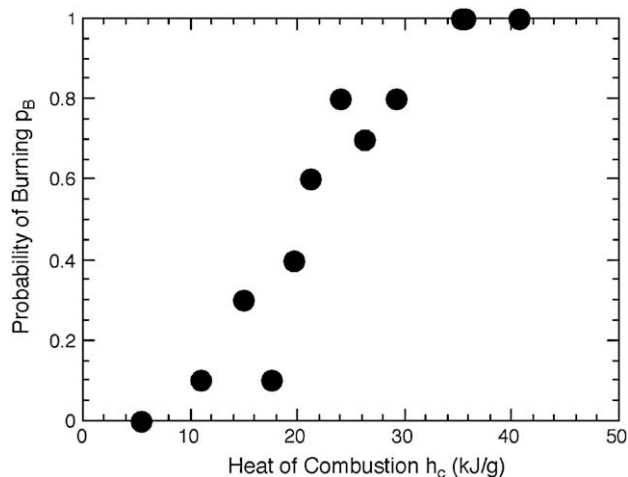


Fig. 11. The probability of burning in the UL 94V test (p_B) versus heat of combustion (h_c) for 110 polymers, plastics and composites.

correlation between η_c and the probability of burning in other standardized flame and fire tests with qualitative (pass/fail) outcomes has been demonstrated [34]. Consequently, η_c and h_c were used to sort and bin the quantitative data for the peak heat release rate in flaming combustion pHRR measured in a fire calorimeter [26] at 50 kW/m² external heat flux.

The pHRR was chosen as the dependent (fire) variable because in the absence of a steady-burning plateau, pHRR is the only time-independent value of the heat release rate measured during the test. In addition, the pHRR is more sensitive to material properties than the average heat release rate [35] and both are calculable from the heat release rate history using a moment-area analysis [36]. Fig. 14 shows the results of the sorting and binning procedure as the average value of pHRR versus the average h_c for 150 polymers, plastics and composites computed for successive 10-sample bins. The data for this subset of the 160-sample flammability database are reasonably well correlated (correlation coefficient, $R = 0.91$) by a proportional relationship with slope 23.8 g/m² s. Fig. 15 shows the results of the sorting and binning procedure for pHRR versus η_c for the 160 polymers, plastics and composites in the flammability database computed for successive 10-sample bins. These data are

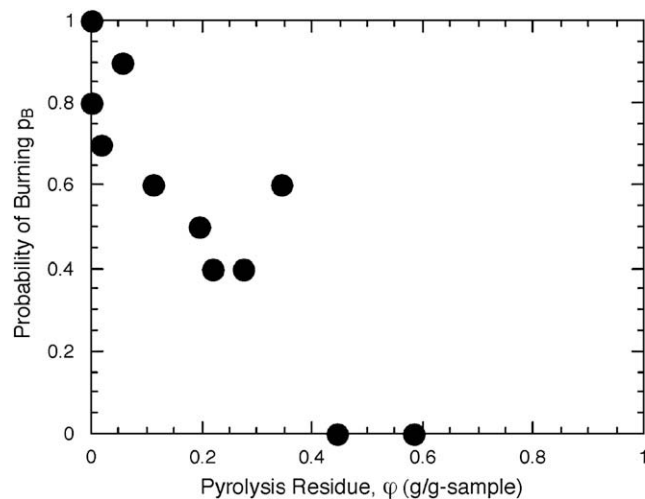


Fig. 12. The probability of burning in the UL 94V test (p_B) versus the pyrolysis residue (φ) for 77 polymers, plastics and composites.

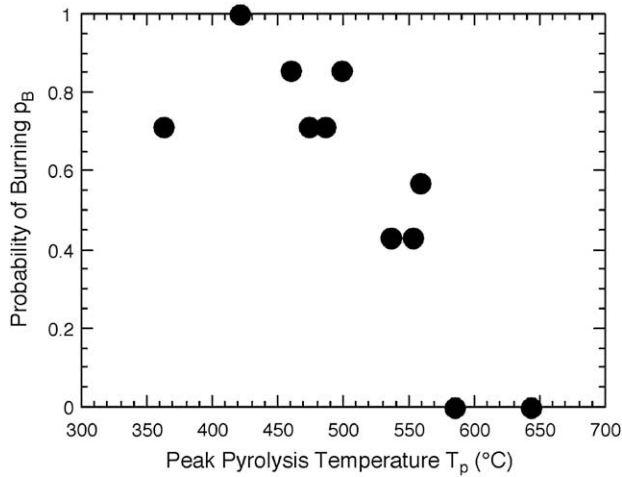


Fig. 13. The probability of burning in the UL 94V test (p_B) versus the temperature at peak pyrolysis rate (T_p) for 77 polymers, plastics and composites.

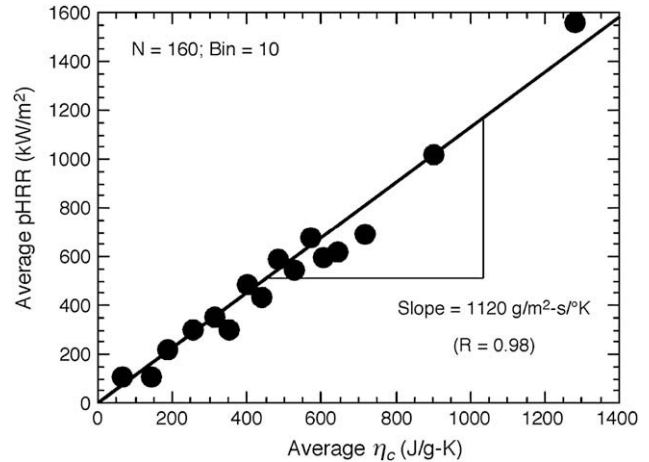


Fig. 15. Peak heat release rate in flaming combustion versus heat release capacity η_c of 160 samples.

very well correlated ($R=0.98$) by a proportional relationship with slope $1120 \text{ g/m}^2 \text{ s/K}$. The ratio of the slopes in Figs. 15 and 14 eliminates pHRR (and any dependence on external heat flux) from the data which, according to Equation (15), gives a global average pyrolysis temperature interval for the 150+ samples, $\Delta T_p = h_c / \eta_c = (1120 \text{ g/m}^2 \text{ s/K}) / (23.8 \text{ g/m}^2 \text{ s}) = 47 \text{ K}$. This value agrees with the approximation (Equation (8)) for a single-step thermal decomposition process having a typical activation energy $E_a = 200 \text{ kJ/mol}$ [1] at a typical polymer pyrolysis/ignition temperature $T_p = 378 \text{ }^\circ\text{C}$ [37], $\Delta T_p = eRT_p^2/E_a = (2.72)(8.314 \text{ J/mol}\cdot\text{K}) - (651 \text{ K})^2 / (200 \text{ kJ/mol}) = 48 \text{ K}$.

The weighted least squares regression lines forced through the origin in Figs. 14 and 15 show good correlation ($R > 0.9$) between pHRR and either h_c or η_c . This fact, and the observation that $\Delta T_p \approx 50 \text{ K}$ over a wide range of polymer composition and properties, allows the energy balance for flaming combustion [38] to be expressed in terms of the thermal combustion properties, $h_c = \eta_c \Delta T_p$ [20–23],

$$\text{HRR} = \chi \frac{h_c}{h_g} (q''_{\text{flame}} - q''_{\text{loss}}) + \chi \frac{h_c}{h_g} q''_{\text{ext}} = \text{HRR}_0 + \frac{\chi \eta_c}{h_g / \Delta T_p} q''_{\text{ext}} \quad (16)$$

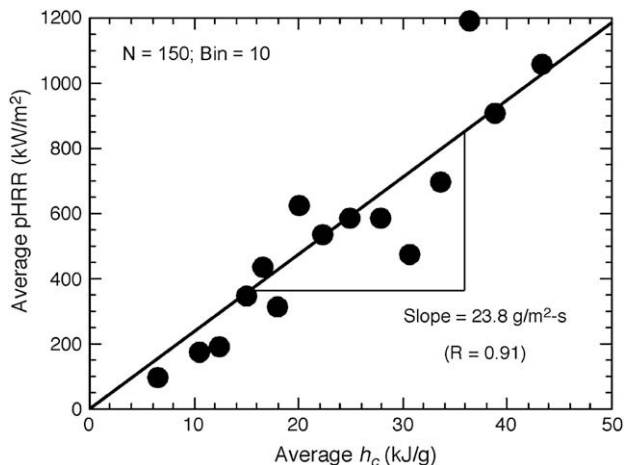


Fig. 14. Peak heat release rate in flaming combustion versus specific heat of combustion h_c of 150 samples.

In Equation (16), χ is the efficiency with which the fuel gases are combusted in the flame, h_g is the energy required to gasify unit mass of solid fuel, q''_{flame} is the heat flux from the flame to the burning surface, $q''_{\text{loss}} \approx \sigma T_p^4$ is the heat loss from the surface due to reradiation with σ the Boltzmann constant, q''_{ext} is the external heat flux from a fire, Bunsen burner, or radiant heater, and HRR_0 is the natural heat release rate of the material in the absence of an external heat flux or Bunsen burner flame [23],

$$\text{HRR}_0 \approx \frac{\chi \eta_c}{h_g / \Delta T_p} (q''_{\text{flame}} - \sigma T_p^4) \quad (17)$$

The apparent proportionality between pHRR, h_c and η_c in Figs. 14 and 15, respectively, is a consequence of the fact that $\chi \eta_c q''_{\text{ext}} / (h_g / \Delta T_p) \gg \text{HRR}_0$ at the high external heat flux, $q''_{\text{ext}} = 50 \text{ kW/m}^2$.

The trends in p_B versus the thermal combustion properties η_c , μ , h_c and T_p for the qualitative data in Figs. 10–13 are consistent with Equations (15)–(17) if there is a heat release rate HRR^* [39] and a corresponding heat release capacity η^* or heat of combustion h^* such that materials are likely to continue burning in the UL 94 test after the Bunsen burner is removed if

$$\frac{\text{HRR}_0}{\text{HRR}^*} = \frac{\eta_c}{\eta^*} = \frac{h_c}{h^*} \geq 1 \quad (18)$$

Figs. 10 and 11 show that sustained burning is likely in the UL 94 vertical flame test ($p_B \geq 0.5$) when $\eta_c \geq 450 \text{ J/g}\cdot\text{K}$ or $h_c \geq 20 \text{ kJ/g}$.

5. Summary and conclusions

The char yield μ , specific heat of combustion h_c , and heat release capacity η_c of engineering plastics were calculated from their chemical structure using additive, empirical molar group contributions. The calculated values for these thermal combustion properties show reasonable agreement with experimental values even though interactions between component chemical groups were neglected. These and other thermal combustion properties were used to sort and compute mean values of qualitative (pass/fail) and quantitative (peak heat release rate) flammability test results using a binning procedure that averages out the random and systematic variations in the dependent variables (fire or flame test results). Of the thermal combustion properties examined, it was found that η_c and h_c best correlate the qualitative flame test results (p_B) and quantitative fire test results (pHRR) and a physical basis for

this observation in terms of the heat release rate in flaming combustion is proposed. A molecular basis for flammability is suggested by the fact that the thermal combustion properties η_c and h_c are rooted in the chemical structure of the polymer.

Acknowledgements

The authors are grateful to Alex Morgan of UDRI, Bernhard Schartel and his group at BAM and Mark Beach of Dow Chemical for sharing their flame resistance and thermal combustion property data for this study, and Sean Crowley (FAA) for the cone calorimeter results. Certain commercial equipment, instruments, materials and companies are identified in this paper in order to adequately specify the experimental procedure. This in no way implies endorsement or recommendation by the Federal Aviation Administration, SRA or General Electric.

References

- [1] Van Krevelen DW. Properties of polymers: their correlation with chemical structure: their numerical estimation and prediction from additive group contributions. 3rd ed. Amsterdam, Netherlands: Elsevier; 1997.
- [2] Cullis CF, Hirschler MM. The combustion of organic polymers. New York, NY: Oxford University Press; 1981.
- [3] Babrauskas V. Comparative rates of heat release from five different types of test apparatuses. *Journal of Fire Sciences* 1986;4:148–59.
- [4] Kashiwagi T, Cleary TG. Effect of sample mounting on flammability properties of intumescent polymers. *Fire Safety Journal* 1993;20:203–25.
- [5] Kashiwagi T. Effect of sample orientation on radiative ignition. *Combustion and Flame* 1982;44:223–45.
- [6] Ritchie SG, Steckler KD, Hamins A, Cleary TG, Yang JC, Kashiwagi T. The effect of sample size on the heat release rate of charring materials, fire safety science. In: Husemi Y, editor. Proceedings of the fifth international symposium. International Association of Fire Safety Science; 1997. p. 177–88.
- [7] Urbas J. Effect of retainer frame, irradiance level and specimen thickness on cone calorimeter test results. *Fire and Materials* 2005;29:1–13.
- [8] Wharton RK. The effect of sample size on the burning behavior of thermoplastic materials in the critical oxygen index test. *Fire and Materials* 1981;5:73–6.
- [9] Walters RN. Molar group contributions to the heat of combustion. *Fire and Materials* 2002;26:131–45.
- [10] Walters RN, Lyon RE. Molar group contributions to polymer flammability. *Journal of Applied Polymer Science* 2003;87:548–63.
- [11] Takemori MT. Group contribution method to predict the flame resistance of polycarbonates, fifth triennial international aircraft fire and cabin safety research conference, Atlantic City, NJ, October 29–November 7; 2007.
- [12] Bicerano J. Prediction of polymer properties. 2nd ed. New York, NY: Marcel Dekker, Inc.; 1996.
- [13] Galiatsatos V, editor. Molecular simulation methods for predicting polymer properties. Hoboken, NJ: John Wiley & Sons; 2005.
- [14] Elzey KA, Ranganathan T, Zilberman J, Coughlin EB, Farris RJ, Emrick T. Novel deoxybenzoin-based polyarylates as halogen-free fire-resistant polymers. *Macromolecules* 2006;39:3553–8.
- [15] Stewart JR. Synthesis and characterization of chlorinated bisphenol-based polymers and polycarbodiimides as inherently fire-safe polymers. Final report DOT/FAA/AR-00/39, Federal Aviation Administration; August 2000.
- [16] Ranganathan T, Zilberman J, Farris RJ, Coughlin EB, Emrick T. Synthesis and characterization of halogen-free antflammable polyphosphonates containing 4,4'-bishydroxy-deoxybenzoin. *Macromolecules* 2006;39:5974–5.
- [17] Ranganathan T, Ku BC, Zilberman J, Beaulieu M, Farris RJ, Coughlin EB, et al. Poly(arylate-phosphonate) copolymers with deoxybenzoin in the backbone: synthesis, characterization, and properties. *Journal of Polymer Science A: Polymer Chemistry* 2007;45:4573–80.
- [18] Benson SW. Thermochemical kinetics: methods for the estimation of thermochemical data and rate parameters. New York, NY: John Wiley & Sons; 1968.
- [19] Yan S, Eddings EG, Palotas AB, Pugmire RJ, Sarofim AF. Prediction of the sooting tendency for hydrocarbon liquids in diffusion flames. *Energy and Fuels* 2005;19:2408–15.
- [20] Lyon RE. Heat release kinetics. *Fire and Materials* 2000;24:179–86.
- [21] Lyon RE, Walters RN, Stoliarov SI. Thermal analysis of flammability. *Journal of Thermal Analysis and Calorimetry* 2007;89:441–8.
- [22] Lyon RE, Walters RN, Stoliarov SI. Screening flame retardants for plastics using microscale combustion calorimetry. *Polymer Engineering and Science* 2007;47(10):1501–10.
- [23] Lyon RE. Plastics and rubber. In: Harper CA, editor. Handbook of building materials for fire protection. New York: McGraw-Hill; 2004. p. 3.1–3.51 [chapter 3].
- [24] Lyon RE, Janssens ML. Polymer flammability. Final report DOT/FAA/AR-05/14. Federal Aviation Administration; May 2005.
- [25] Wilkie CA, Chigwada G, Gilman JW, Lyon RE. High-throughput techniques for the evaluation of fire retardancy. *Journal of Materials Chemistry* 2006;16:2023–30.
- [26] Schartel B, Pawlowski KH, Lyon RE. Pyrolysis-combustion flow calorimeter: a tool to assess flame retarded PC/ABS materials. *Thermochimica Acta* 2007;462:1–14.
- [27] Morgan AB. Micro combustion calorimeter measurements on flame retardant polymeric materials. In: Proceedings of the Society for the Advancement of Materials and Process Engineering (SAMPE) Fall technical conference, Cincinnati, OH, October 29–November 1, 2007.
- [28] Lin TS, Cogen JM, Lyon RE. Correlations between microscale combustion calorimetry and conventional flammability tests for with halogen-free flame retardant polyolefin compounds. *Fire and Materials* 2009;33:33–50.
- [29] Standard test method for determining flammability characteristics of plastics and other solid materials using microscale combustion calorimetry, ASTM D 7309-07. West Conshohocken, PA: American Society for Testing and Materials (International); April 1, 2007.
- [30] Flammability of plastic materials. Northbrook, IL: Underwriters Laboratories Inc.; 1991. UL 94 Section 2 (Horizontal: HB) and Section 3 (Vertical: V-0/1/2).
- [31] Standard test method for measuring the comparative burning characteristics of solid plastics in a vertical position, ASTM D 3801-06. West Conshohocken, PA: American Society for Testing and Materials (International); 2006.
- [32] Standard test method for heat and visible smoke release rates for materials and products using an oxygen consumption calorimeter, ASTM E 1354. West Conshohocken, PA: American Society for Testing and Materials; 2004.
- [33] Lyon RE, Walters RN, Castelli LA. Fire resistant polymers based on bisphenol-C. Proceedings of the Society for the Advancement of Materials and Process Engineering annual conference, SAMPE 2004, Long Beach, CA, May 17–20; 2004.
- [34] Lyon RE, Safronava N, Walters RN, Stoliarov SI. A statistical model for the results of flammability tests. *Fire and Materials* 2009, San Francisco, CA, Jan. 26–28, 2009.
- [35] Stoliarov SI, Safronava N, Crowley S, Lyon RE. The effect of polymer properties on burning rate, building and fire research laboratory annual fire conference. Gaithersburg, MD: National Institute of Standards and Technology; April 27–30, 2009.
- [36] Lyon RE, Crowley S, Walters RN. Steady heat release rate by the moment area method. *Fire and Materials* 2008;32:199–212.
- [37] Babrauskas V. Ignition handbook. Issaquah, WA: Fire Science Publishers; 2003. p. 241.
- [38] Tewarson A. Flammability parameters of materials: ignition, combustion and fire propagation. *Journal of Fire Sciences* 1994;12:329–56.
- [39] Lyon RE, Quintiere JG. Piloted ignition of combustible solids. *Combustion and Flame* 2007;151:551–9.